Very High Single Channel Water Permeability of Aquaporin-4 in Baculovirus-Infected Insect Cells and Liposomes Reconstituted with Purified Aquaporin-4[†]

Baoxue Yang, Alfred N. van Hoek, and A. S. Verkman*

Departments of Medicine and Physiology, Cardiovascular Research Institute, University of California, San Francisco, California 94143-0521

Received January 30, 1997; Revised Manuscript Received March 19, 1997[⊗]

ABSTRACT: The insect cell/baculovirus system was used to express the mercurial-insensitive water channel aquaporin-4 (AQP4) for purification and reconstitution. Immunoblot analysis of Sf9 cells infected with recombinant baculovirus showed greatest AQP4 expression at 72 h after infection at a multiplicity-of-infection of 5. Immunostaining and cell membrane fractionation indicated AQP4 plasma membrane expression. Quantitative immunoblot analysis showed ∼60 μg of AQP4 per milligram of plasma membrane protein (∼2 mg of AQP4 protein per liter of Sf9 cell culture). Functional analysis by stopped-flow light scattering indicated that AQP4 functioned as a mercurial-insensitive water-selective transporter. Osmotic water permeability (P_f) in plasma membrane vesicles from AQP4-expressing Sf9 cells was very high (0.053 cm/s at 10 °C), weakly temperature dependent (activation energy, 4.5 kcal/mol), and not inhibited by $HgCl_2$. The AQP4 single channel water permeability (p_f), estimated from P_f and protein amount, was 19×10^{-14} cm^3/s. Purification of AQP4 to a single Coomassie blue-stained protein on SDS−PAGE (1300-fold over homogenate) was achieved by membrane fractionation, carbonate stripping of nonintegral proteins, solubilization in octyl-β-glucoside, and anion exchange chromatography. AQP4 protein identity was confirmed by mass spectrometry. Reconstitution of purified AQP4 into proteoliposomes increased osmotic water permeability by >40-fold, giving a p_f of 15×10^{-14} cm^3/s, remarkably greater than that of 4.9×10^{-14} cm^3/s measured in parallel for AQP1. These results establish the first purification of an aquaporin from a heterologous expression system. The high AQP4 p_f suggests (a) significant functional differences among the aquaporins, (b) inadequacy of existing pore models to account for high water flow and water permselectivity, and (c) possible enhancement of water flow by AQP4 assembly in orthogonal arrays.

A family of water-transporting proteins (water channels or aquaporins) has been identified which are expressed in fluid-transporting tissue in mammals, amphibians, plants, and bacteria (reviewed in references *1*−*4*). The molecular water channels are small (∼30 kDa) hydrophobic proteins with homology to the major intrinsic protein (MIP) of lens fiber (*5*). It has been proposed that the water channels have a physiological role in fluid-transporting cells. However, a physiological role has thus far been established only for aquaporin-2 (AQP2), the apical membrane water channel of kidney collecting duct (*6*), which is required for vasopressin-regulated water permeability and formation of concentrated urine (*7*). Aquaporins-3 and -4 are constitutively expressed at the basolateral membrane of the same cells expressing AQP2 (*8*), and may provide a route for water exit from principal cells. Water channels have also been localized to selected epithelial and endothelial cell plasma membranes in lung, brain, eye, intestine, exocrine glands, and other organs that carry out vectorial fluid transport.

A substantial amount of information about aquaporin-1 (CHIP28, AQP1) structure and function has been obtained because AQP1 can readily be purified in quantities of tens of milligrams from erythrocyte plasma membranes. AQP1 forms heterotetramers in membranes (*9*, *10*) containing a 1:1 mixture of glycosylated and nonglycosylated monomers (*11*). Each monomer appears to function independently as a water-selective channel (*12*). Structural studies of two-dimensional crystals of human AQP1 in reconstituted proteoliposomes by electron cryocrystallography (*13*) and of glucose-preserved membranes by electron crystallography (*14*, *15*) suggest that each AQP1 monomer contains six helical domains that span the bilayer with a putative aqueous pore at the center. None of the other aquaporins have been purified from native tissues, nor have they been expressed heterologously in significant quantities.

AQP4 has unique characteristics compared to other aquaporins—AQP4 water permeability is not inhibited by mercurials (*16*, *17*), and the AQP4 protein spontaneously forms crystalline orthogonal arrays of particles (OAPs) in membranes (*18*). From prior considerations on water flow mechanisms (*19*), it was proposed that OAPs might increase water flow by enhancing bulk flow in the vicinity of OAPs. Although a considerable body of information exists on AQP4 genetics (*20*), tissue distribution (*8*, *21*), and biogenesis (*22*), including the recent generation of a transgenic AQP4 knock-out mouse (*23*), there is no suitable native tissue source for

[†] This work was supported by Grants DK35124 and HL42368 from the National Institutes of Health and Grant R613 from the National Cystic Fibrosis Foundation.

* Address correspondence to this author at 1246 Health Sciences East Tower, Cardiovascular Research Institute, University of California, San Francisco, San Francisco, California 94143-0521. Phone: (415)-476-8530; Fax: (415)-665-3847. E-mail: verkman@itsa.ucsf.edu.

[⊗] Abstract published in *Advance ACS Abstracts,* June 1, 1997.

S0006-2960(97)00231-6 CCC: $14.00

AQP4 purification. The purpose of this study was to develop a heterologous expression system and AQP4 purification method to test the hypothesis that the intrinsic (per channel, or *single channel*) water permeability of AQP4 is greater than that of AQP1, which does not form OAPs (*9*). Based on work that functional AQP1 water channels were expressed in yeast (*24*), we initially evaluated the Pichia expression system (*35*); however, although AQP4 was expressed and was functional in spheroplasts, only tens of micrograms could be generated per liter of culture. We report here that baculovirus-infected Sf9 cells express functional AQP4 water channels strongly at the cell plasma membrane, producing water permeabilities that were substantially higher than those found in any mammalian tissue. The expression system was optimized, AQP4 function was characterized, and purification to a single Coomassie blue-stained protein on SDS−PAGE was accomplished under nondenaturing conditions by membrane fractionation, high-pH stripping, detergent solubilization, and anion chromatography. The identity of the purified AQP4 was confirmed by mass spectrometry, and the protein functioned as a water channel when reconstituted into liposomes with a single channel water permeability ~3-fold greater than that for AQP1.

METHODS

Construction of Recombinant Baculovirus. Full-length cDNA encoding rat AQP4 (*16*, *26*) was PCR-amplified using the primers sense (5′-GAAGATCTGCCATGGTGGCTTTCAAAGGCGTC-3′) and antisense (5′-CCCAAGCTTATACAGAAGATAATACCTCTCCA-3′). The primers contain engineered *Bgl*II and *Hind*III restriction sites (underlined) for insertion into pBlueBac4 (Invitrogen). A rat AQP4 fusion protein containing a polyhistidine, tag $(his)_6$, at the N-terminus was constructed by subcloning the same insert into pBlueBacHis (Invitrogen). Recombinant virus was generated by cotransfecting each of the plasmids with linearized wild-type AcMNPV viral DNA using cationic liposomes according to the manufacturer's protocol (Invitrogen). Plaques containing AQP4 recombinant virus were identified by a blue color after 5−7 days using plates containing 0.15 mg/mL X-gal. After two rounds of plaque purification, the recombinant virus was amplified, and the presence of AQP4 cDNA and the absence of contaminating wild-type virus were confirmed by PCR using primers corresponding to sequences in pBlueBac4 flanking the insert.

Sf9 Cell Culture and Infection. For production of recombinant proteins, Sf9 (*Spodoptera frugiperda*) cells [$(1.5-2.0) \times 10^6$/mL, Invitrogen] were generally infected at a multiplicity-of-infection (MOI) of 5 and harvested at 72 h. Sf9 cells were maintained at 27 °C in Grace's insect medium supplemented with 10% fetal bovine serum and 10 μg/mL gentamicin (Gibco BRL). Suspension cultures were maintained in 500 or 1000 mL spinner flasks and stirred at a rate of 80 rpm.

Subcellular Fractionation. At 72 h postinfection, 6×10^8 cells (from 400 mL of culture) were pelleted at 100*g* for 10 min, and washed twice in ice-cold homogenizing buffer (HB: 250 mM sucrose, 10 mM Tris-HCl, pH 7.4). The pellet was resuspended in HB containing antipain (1 μg/mL), pepstatin (1 μg/mL), leupeptin (1 μg/mL), phenylmethanesulfonyl fluoride (20 μg/mL), and 1 mM EDTA, and homogenized by 20 strokes of a glass Dounce homogenizer. The homogenate was centrifuged at 500*g* for 10 min at 4 °C, and the supernatant was adjusted to 1.4 M sucrose, 10 mM Tris-HCl (pH 7.4), and 0.2 mM EDTA. A discontinuous sucrose gradient [2 M sucrose (3 mL), 1.6 M (6 mL), 1.4 M (12 mL, containing homogenate), 1.2 M (12 mL), 0.8 M (3 mL)] was centrifuged for 2.5 h at 25 000 rpm in an SW 28 rotor (Beckman), and fractions were collected. Protein concentration was determined by Bio-Rad Protein Assay, and marker enzyme activities (α-mannosidase and alkaline phosphodiesterase I) were measured as reported previously (*27*).

Water Transport Assay. Osmotic water permeability (P_f) was measured by stopped-flow light scattering (*28*) in vesicle fractions suspended at ~0.5 mg of protein/mL in 50 mM sucrose, 10 mM Tris-HCl, pH 7.4, and in proteoliposomes (see below). Vesicles were subjected to a 100 mM inwardly-directed sucrose gradient and the time course of scattered light intensity at 530 nm was measured. P_f was computed from the light scattering time course and vesicle size.

Immunoblot Analysis. Protein samples were electrophoresed on a 12% SDS-polyacryamide gel and electroblotted onto a poly(vinylidene difluoride) membrane. The membrane was incubated with a 1:1000 dilution of immune or preimmune serum containing a rabbit anti-rat AQP4 antibody directed against a synthetic C-terminal peptide (amino acids 287−301, EKGKDSSGEVLSSV) of the deduced rat amino acid sequence (*8*). Blots were washed in PBS, incubated with an alkaline phosphatase-conjugated goat anti-rabbit IgG antibody (1:3000, Life Technologies, Inc.), and developed with 5-bromo-4-chloro-3-indolylphosphate (16 μg/mL) and nitroblue tetrazolium (0.33 μg/mL).

Immunofluorescence. Sf9 cells cultured on glass coverslips were fixed in 4% paraformaldehyde in PBS containing 0.1 M sucrose for 20 min. Cells were permeabilized with 0.5% Triton X-100 for 10 min at 23 °C, and then incubated with a 1:500 dilution of anti-AQP4 immune serum for 1 h. Slides were rinsed three times with PBS and incubated for 30 min with a fluorescein-conjugated goat anti-rabbit IgG (Boehringer) (1:50) in PBS containing 1% BSA. Slides were washed three times with PBS and covered with Dabco (diazabicyclooctane) solution and a glass coverslip.

Protein Purification. The starting material for AQP4 purification was the plasma membrane pellet (fractions 5 and 6) isolated as described above. A series of membrane stripping procedures and detergents were tested initially for their ability to extract AQP4 and total protein from membranes (see Results). Stripping was accomplished by 1 h incubations of 50 μL of membrane suspension (~5 mg of protein/mL) at 23 °C in one of the following: 3.5 M urea, 1 M KI, 1 M KSCN, 0.1 M HCl, 0.1 M Na_2CO_3, or 0.1 M NaOH. Detergent treatments consisted of a 1 h incubation of carbonate-stripped membranes with one of the following: 10% heptyl, octyl, or nonyl β-D-glucoside, nonyl, decyl, or dodecyl-β-D-maltoside; Cymal [4-(cyclohexyl)butyl-β-D-maltoside]; MEGA 8 (octanoyl-*N*-methylglucamide); HEGA-8 [octanoyl-*N*-(hydroxyethyl)glucamide] (each from Anatrace); *N*-lauroylsarcosine; SDS (Sigma); cholate or deoxycholate (Fluka). Membranes were pelleted by centrifugation of the 50 μL suspensions in an AirFuge (Beckman) at 25 psi (165000*g*) for 30 min. Protein concentrations were determined by the Lowry assay in the presence of SDS. Samples were electrophoresed in 12% Laemmli gels for

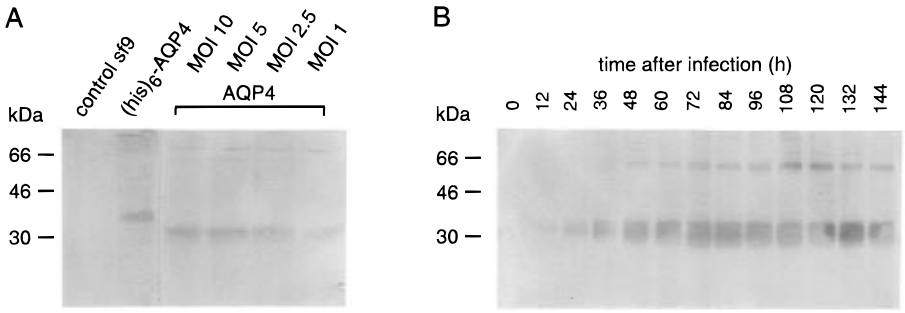

FIGURE 1: Expression of AQP4 protein in baculovirus-infected Sf9 cells. Immunoblot probed with anti-AQP4 antibody. Sf9 cell membrane homogenates (10 μg of protein/lane) were resolved by SDS−PAGE, electroblotted, and probed as described under Methods. (A) Lanes contain control (uninfected) Sf9 cells, $(his)_6$AQP4−Sf9 cells expressing the his-tagged AQP4 fusion protein, and AQP4−Sf9 cells infected at the indicated MOIs. (B) Time course of AQP4 expression after baculovirus infection at an MOI of 5.

Coomassie and silver staining (NOVEX), and immunoblot analysis.

Larger scale preparations of AQP4 (from 2 L cultures of baculovirus-infected Sf9 cells) were subjected to carbonate stripping and OG solubilization (at 100 mM OG), and further purified by anion-exchange chromatography with Q-Sepharose (Pharmacia). An open column (0.5 cm diameter × 2 cm length), containing 300 mL of resin, was preequilibrated with 35 mM OG, 4 mM Tris-HCl (pH 7.4), and 30 mM NaCl. The OG-solubilized protein was applied, and the flow through was collected and reapplied onto a second column. The column was washed with 10 volumes of equilibration buffer and then stepwise-eluted with 3 column volumes of the OG/Tris buffer containing progressively increasing [NaCl].

Mass Spectrometry. A 4.5 μg sample of the anion exchange-purified AQP4 was digested with sequencing grade trypsin in 0.1 mM HCl at 23 °C for 2 h. Peptides were desalted on C_{18} reverse-phase HPLC, and loaded onto an RP-300 C_{18} column (7 μm bead size, Applied Biosystems International) preequilibrated with 98% solvent A (98:1.9:0.1 water/acetonitrile/trifluoroacetic acid) and 2% solvent B (5:95:0.09). Chromatography was done on an ultrafast microprotein analyzer (flow rate 50 μL/min). Peptides were eluted following a step to 50% solvent A/50% solvent B. Fractions corresponding to protein peaks (identified by 210 nm absorbance) were dried and dissolved in 50% acetonitrile, 5% trifluoroacetic acid, and water. The solution was diluted 1:10 in water and mixed with an equal volume of α-cyano-4-hydroxycinnamic acid matrix-assisted laser desorption ionization (MALDI) matrix, and 1 μL was dried onto the mass spectrometer target probe. Molecular masses were obtained using a TofSpec SE mass spectrometer (MicroMass) equipped with a reflectron and nitrogen laser (337 nm). Data were collected as positive ion spectra, and calibrated using external peptide standards. For post-source decay (PSD) sequence analysis, selected peaks were focused by stepping the reflectron voltage and spectra recorded.

Protein Reconstitution. A mixture of 0.2 mg L-α-dipalmitoylphosphatidylcholine, 0.1 mg of L-α-phosphatidylethanolamine (Sigma), 0.02 mg of phosphatidylinositol (Avanti), and 0.12 mg of cholesterol in chloroform/ether was dried and hydrated with 20 mL of 0.1 M sodium phosphate (pH 7.4) and 2.5 mM EDTA. The suspension was centrifuged for 1 h at 20 000 rpm (SS-34 rotor, Sorvall), washed, and resuspended in 5 mL of 0.1 M sodium phosphate (pH 7.4), 1 mM EDTA. For reconstitution, 100 μL of the lipid mixture (80 mg/mL) was 10-fold-diluted with water (25 °C) containing 100 mM OG. Complete solubilization of the lipids was achieved after 5 min of incubation. Lipids (0.8 mg) and protein (0−0.05 mg) were mixed and dialyzed against 10 mM sodium phosphate (pH 7.4), 0.1 mM EDTA for 6 h at 23 °C, followed by 6 h at 0 °C, utilizing a SpectraPor dialysis membrane with molecular mass cutoff of 6000−7000 daltons. In some experiments, 2 mM DDT was added to the protein solution 30 min prior to and during the dialysis. Control experiments were carried out by the same procedure in the absence of protein, and with purified AQP1 (prepared as described in reference *11*) in place of AQP4. The vesicle diameter for the AQP4 and AQP1 proteoliposomes and for the liposomes was determined by quasi-elastic light scattering to be in the range 140−180 nm. Single channel water permeability coefficients (p_f, cm^3/s) were computed from the protein-to-lipid ratio and proteoliposome water permeability as described previously (*28*).

RESULTS

Initial experiments were carried out to determine whether functional AQP4 could be expressed in Sf9 cells and to optimize the level of AQP4 protein expression. Recombinant baculoviruses encoding AQP4 or a $(his)_6$AQP4 fusion protein were isolated by serial plaque assays and used to infect Sf9 cells. Figure 1 shows an immunoblot of Sf9 cell membrane homogenates probed by an anti-AQP4 antibody raised against a synthetic C-terminal peptide. No protein was detected in uninfected Sf9 cells or just after infection with baculovirus encoding AQP4. A band at ∼32 kDa was observed by 24 h after infection and was strong by 72 h. Often a second band at ∼64 kDa was observed depending upon sample handling; this larger band corresponds to an AQP4 dimer (*21*, *22*). AQP4 is a very hydrophobic protein that can form dimers and higher order oligomers even in SDS. No AQP4 glycosylation was found, similar to results in native tissues (*8*, *21*). No positive bands were detected in a parallel blot probed by AQP4 immune serum containing a >100-fold molar excess of the AQP4 C-terminal peptide (not shown). Less AQP4 expression was found at lower MOIs of 1 and 2.5, whereas higher MOIs produced more cellular destruction and protein degradation by released proteases. The protein size from Sf9 cells expressing the $(his)_6$AQP4 fusion protein was slightly greater because of the additional 37 amino acids (6 histidines and linker containing enterokinase cleavage site, predicted size 34.4 kDa) at the AQP4 N-terminus.

Immunostaining and cell fractionation were done to determine the cellular distribution of AQP4 in Sf9 cells at 72 h after baculovirus infection at an MOI of 5. High

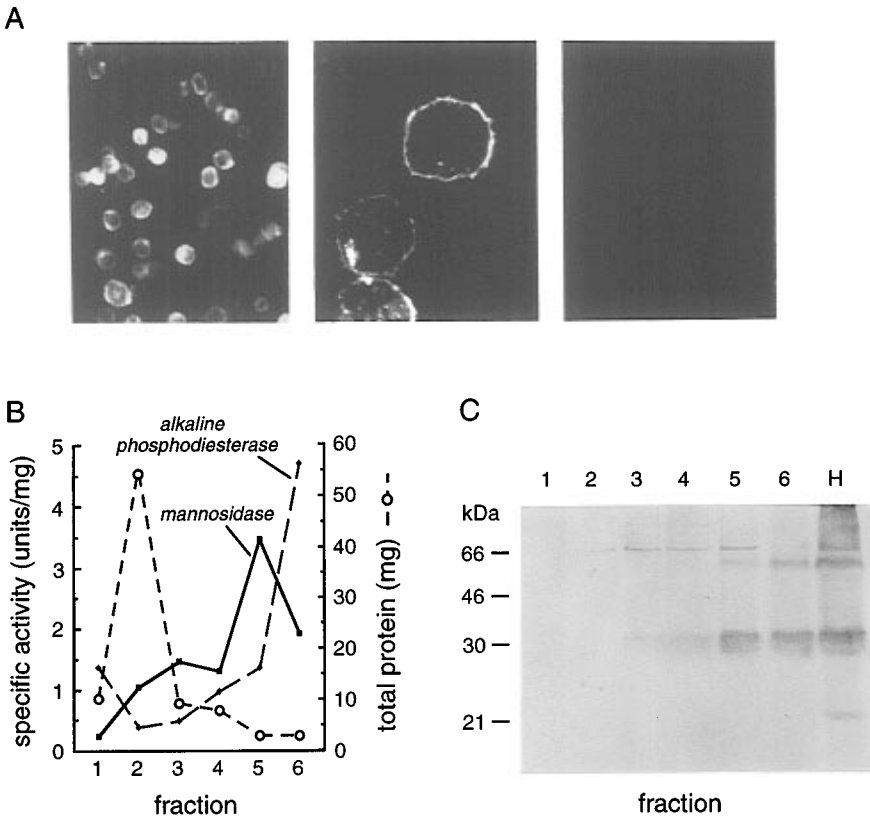

FIGURE 2: Cellular distribution of AQP4 protein expression. Sf9 cells were infected with the AQP4 baculovirus for 72 h. (A) Immunostaining with anti-AQP4 antibody at low magnification (left) and by high magnification confocal microscopy (middle). Control Sf9 cells shown at the right. (B) Fractionation of Sf9 cell membranes by sucrose gradient centrifugation. Protein concentrations and enzyme activities for mannosidase (a Golgi marker in Sf9 cells, reference *38*) and alkaline phosphodiesterase (a plasma membrane marker) of six pooled fractions. (C) Immunoblot of membrane fractions probed by anti-AQP4 antibody. Lanes contain 10 μg of membrane protein.

magnification confocal microscopy (Figure 2A, middle; left for low magnification) suggested AQP4 expression primarily in a plasma membrane distribution, although possible Golgi staining near the plasma membrane is not evaluated well by light microscopy. Control Sf9 cells stained in parallel showed no immunofluorescence (Figure 2A, right), nor did AQP4-expressing Sf9 cells incubated with anti-AQP4 antiserum containing excess AQP4 C-terminal peptide (not shown). Measurement of water permeability in the intact Sf9 cells by stopped-flow light scattering was unsuccessful because of the large cell size which resulted in cell trauma during the high-shear mixing.

To assay water transport function and as an initial step in purification, AQP4 cell membranes were fractionated by a sucrose gradient centrifugation procedure used previously for CHO cells (*27*). Eighteen fractions were collected and pooled into six fractions. Protein and marker enzyme assays indicated that the vast majority of membrane protein was in fraction 2 (Figure 2B), which contained mostly endoplasmic reticulum vesicles. Fraction 6 contained mostly plasma membrane vesicles, whereas fraction 5 contained Golgi and plasma membrane vesicles. Immunoblot analysis of the vesicle fractions showed AQP4 expression in fractions 5 and 6 (Figure 2C), indicating AQP4 expression in Golgi and plasma membranes.

Functional measurements of osmotic water permeability were carried out in the isolated vesicle fractions by stopped-flow light scattering. Vesicles were subjected to a 100 mOsm inwardly-directed osmotic gradient, and the time course of 90° scattered light intensity was measured. Figure

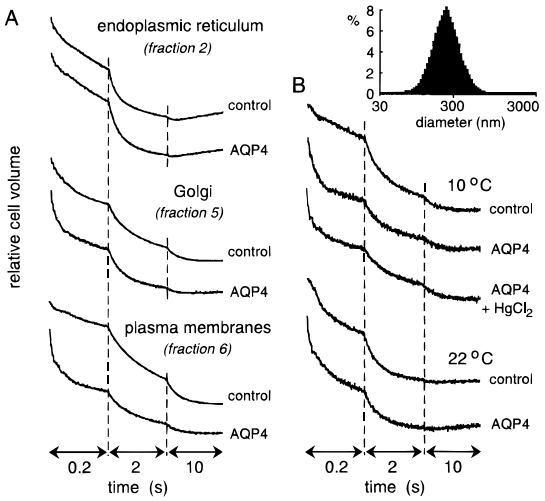

FIGURE 3: Measurement of osmotic water permeability in membrane fraction by stopped flow light scattering. Vesicles (0.5−1 mg of membrane protein/mL) were subjected to a 100 mOsm inwardly directed osmotic gradient. A. Comparison of water permeabilities in indicated membrane fractions from control and AQP4-expressing Sf9 cells. (B) Temperature dependence of water permeability in the plasma fraction from AQP4-expressing cells. Where indicated, 0.3 mM $HgCl_2$ was present. Inset: Size distribution of vesicles in fraction 6 measured by quasi-elastic light scattering.

3A shows a comparison of light-scattering data for vesicle fractions isolated from control and AQP4-expressing Sf9 cells. Whereas no difference in the time course of vesicle shrinkage was found for the endoplasmic reticulum-derived vesicles (fraction 2), there was an increased rate of shrinkage

Table 1: Purification of AQP4 Protein from Sf9 Cells[a]

	total protein (mg)	AQP4 (mg)	yield (%)	purification ratio
cell homogenate	2700	2.1	100	1.0
postnuclear supernatant	427	1.8	86	5.5
plasma membrane fractions 5+6	8.1	0.48	23	78
carbonate-stripped membranes	4.8	0.44	21	119
OG solubilized material	2.0	0.42	20	270
anion exchange chromatography	0.11	0.11	5	1300

[a] Protein amounts are reported per liter of Sf9 cell culture harvested at 72 h after infection with recombinant AQP4 baculovirus at an MOI of 5. Total protein concentrations were determined by the Lowry procedure and AQP4 protein by quantitative immunoblot analysis.

in fractions 5 and 6 from the AQP4-expressing cells. Osmotic water permeability for the fraction 6 vesicles determined from the light-scattering time course and an average vesicle diameter of 270 nm (measured by quasi-elastic light scattering, see Figure 3 inset) was 0.053 ± 0.006 cm/s (SE, 3 preparations) at 10 °C. This value is remarkably greater than that reported in native cell membranes expressing water channels such as erythrocytes (P_f 0.02 cm/s), kidney proximal tubule vesicles (0.015 cm/s), and endosomes from kidney collecting duct containing the vasopressin-sensitive water channel (0.02 cm/s) (4). Figure 3B shows that water permeability in the AQP4-expressing cells was temperature-dependent and not inhibited by $HgCl_2$. The Arrhenius activation energy computed from P_f values was 4.5 kcal/mol. This value is similar to that of 3.6 kcal/mol reported for *Xenopus* oocytes expressing rat AQP4 (*16*). Stopped-flow measurements with 100 mM gradients of urea and glycerol showed little solute entry over 30 s (not shown), indicating that AQP4 is permselective for water.

Purification of the AQP4 protein was carried out. The amount of AQP4 protein and purification ratios for each step are summarized in Table 1. The starting material for purification was combined fractions 5 and 6, which contained the majority of AQP4 protein and already gave a 78-fold purification relative to total Sf9 cell protein. The next purification step was membrane stripping of nonintegral proteins. Membranes were incubated in a series of agents that have been used to remove nonintegral proteins. After incubation and centrifugation, pellets and supernatants were assayed for total protein and AQP4. As seen by immunoblot analysis (Figure 4A), incubations with KSCN, carbonate, and NaOH effectively stripped protein without significant loss of AQP4 from the pellet. Carbonate-stripped membranes (in which AQP4 water permeability was not affected, data not shown) were used to identify detergent(s) that could solubilize AQP4 effectively. A series of nondenaturing detergents were tested as shown in Figure 4B. Again, membranes were incubated with each detergent, and centrifuged to obtain pellets and supernatants for analysis of total protein and AQP4. AQP4 was effectively solubilized by several detergents. For subsequent purification procedures, the membrane pellet was solubilized in OG because this nondenaturing detergent dissolves 100% of the AQP4 protein but only ~40% of total protein (giving 270-fold AQP4 purification over Sf9 cell homogenate), and is suitable for anion exchange chromatography and reconstitution as was done for AQP1 (Van Hoek et al., 1993). Figure 5A shows a Coomassie blue-stained gel and Figure 5B the corresponding immunoblot for the carbonate stripping and OG solubilization procedures. A strong enrichment of immunoreactive AQP4 protein relative to total protein is seen.

The OG-solubilized material was subjected to anion exchange chromatography using a small open column containing Q-Sepharose. Following application of 2 mL to 300 μL of resin, the flow through did not contain appreciable amounts of AQP4 but did contain several proteins including an impurity (seen as a sharp band at ~32 kDa) that migrated in the same region as AQP4 (Figure 5A, lane 6). This impurity, which was not recognized by the AQP4 antibody (Figure 5B), was further removed by elution with 30 mM NaCl (lane 7). Elution with 150 mM NaCl gave several proteins, including a major remaining impurity of 25 kDa, with little elution of immunoreactive AQP4 (weak immunostained band in lane 8). AQP4 was subsequently eluted at higher salt concentrations. The Coomassie-stained gel showed purification of AQP4, seen as a fuzzy band at ~31 kDa (and minor dimer/tetramer bands as discussed above) (lane 9). Quantitative densitometry of a silver-stained gel indicated AQP4 purification to >96%.

Figure 6 shows an immunoblot of homogenates and membranes prepared during the purification procedure, and Table 1 summarizes enrichment ratios and yields. The figure shows progressive enrichment of the AQP4-immunoreactive protein. Dilution analysis of the purified protein indicated that the polyclonal antibody could detect 6 ng of the pure protein. The amount of AQP4 purified per liter of Sf9 cell culture was 0.11 mg, representing a final purification factor of 1300 over the original Sf9 cell homogenate. To confirm that the purified protein was AQP4, mass spectrometry analysis was carried out on the protein eluted at high salt from the anion exchange column (see Methods). After trypsin digestion, major molecular ions were observed at mass-to-charge (m/z) ratios of 2904.8 and 3032.5, corresponding to the theoretical AQP4 tryptic peptides, ^{285}Ser−Lys^{310} and ^{285}Ser−Lys^{311}, respectively. Analysis of the molecular ion at 2904.8 by MALDI-PSD gave fragment ions at m/z 604.5, 833.2, 2117.9, 2462.1, 2631.5, and 2779.0. A full search of the MS-Tag database with these masses indicated that they correspond exactly to the ^{285}Ser−Lys^{310} peptide of rat AQP4 and to no other protein in the database.

The purified protein was reconstituted into proteoliposomes for measurement of water permeability. In response to an osmotic gradient, liposomes containing no protein shrank slowly with a half-time of ~500 ms (Figure 7, top). In initial experiments, there was little increase in water permeability in AQP4 proteoliposomes prepared by the protocol used previously for AQP1. There was little influence of lipid composition, including the use of brain lipid extracts in place of the defined lipid mixture. However, reconstitution under reducing conditions gave proteoliposomes of the same size as those formed in the absence of DTT, but with very high water permeability (half-time 11−14 ms, Figure 7, middle), higher than that in proteoliposomes reconstituted with similar amounts of the AQP1 protein (Figure 7, bottom). The slower signal decrease over >1 s probably represents shrinkage of large multilamellar contaminating liposomes. P_f in AQP4-containing proteoliposomes was weakly temperature-dependent (activation energy 3.0 kcal/mol) and not inhibited by 0.3 mM $HgCl_2$. The averaged single channel AQP4 water permeability, computed from the proteoliposome P_f (determined by analysis of the curve over the first second) and the protein-to-lipid ratio,

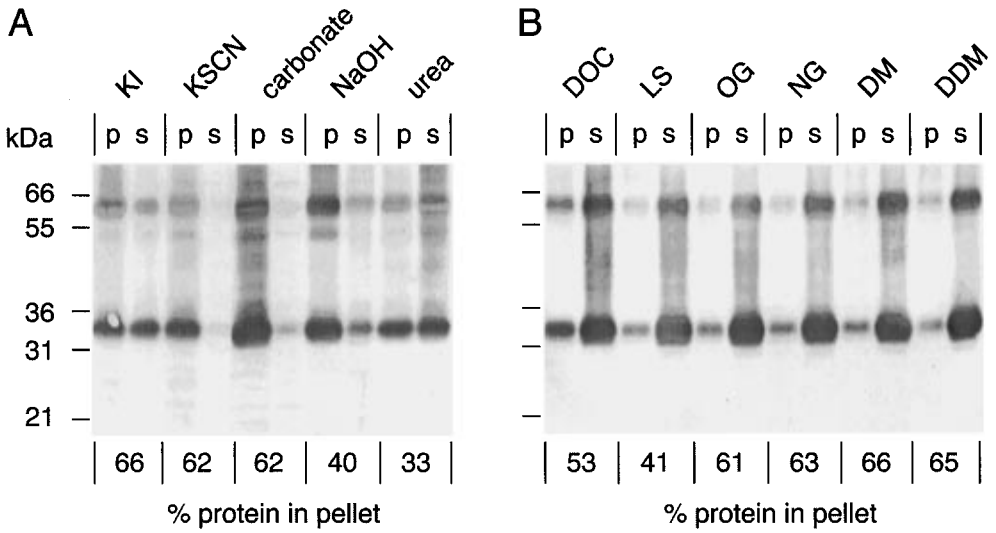

FIGURE 4: Stripping and solubilization of AQP4-containing membranes. Immunoblots probed with AQP4 antibody are shown. Plasma membranes (fractions 5 and 6) were treated with stripping agents (A) or detergents (B) and centrifuged as described under Methods. Proteins in the pellets (p) and supernatants (s) were resolved by SDS−PAGE and blotted. The percentage of total protein in the pellet is shown at the bottom for each maneuver. See text for details.

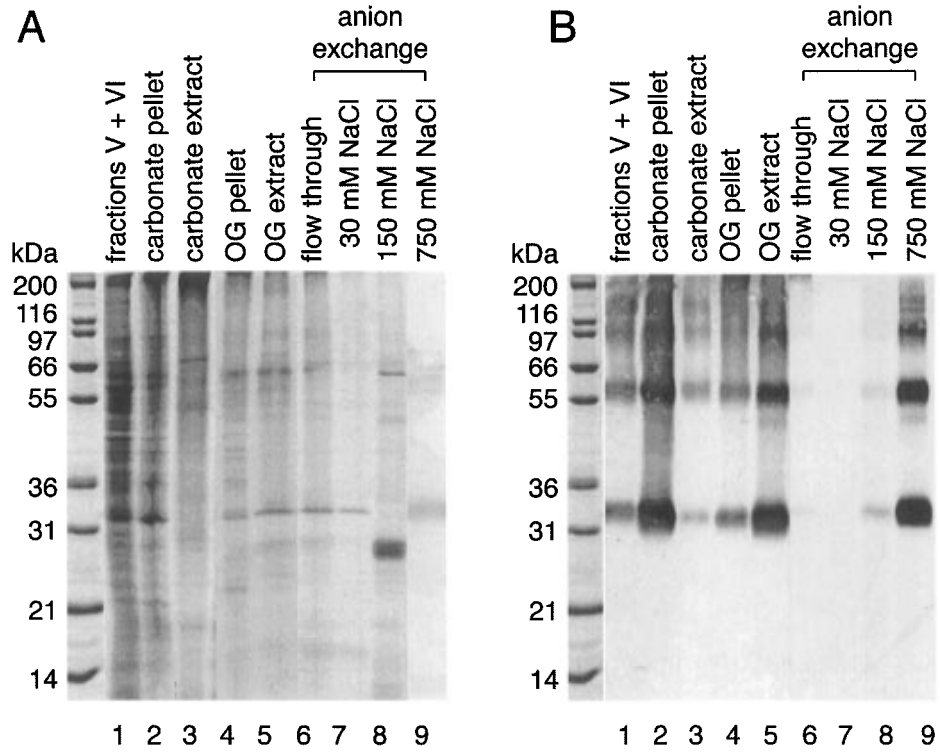

FIGURE 5: Purification of AQP4 from baculovirus-infected Sf9 cells showing Coomassie blue-stained gel (A) and corresponding immunoblot probed with AQP4 antibody (B). Lanes contained: (1) plasma membrane fractions (30 μg), (2) pellet after carbonate stripping (20 μg), (3) supernatant after carbonate stripping (10 μg), (4) pellet after OG solubilization (10 μg), (5) supernatant after OG solubilization (10 μg), (6) flow through from the anion exchange column, and (7−9) protein eluted from the anion exchange column at the indicated [NaCl].

was $(15 \pm 3) \times 10^{-14}$ cm^3/s ($n = 3$) at 10 °C, a value significantly greater than that of $(4.9 \pm 1) \times 10^{-14}$ cm^3/s for AQP1 (see Discussion).

DISCUSSION

The purpose of this study was to obtain purified, functional AQP4 for measurement of single channel permeability properties. Because AQP4 isolation from native tissues was not possible, the insect cell−baculovirus system was established for heterologous expression and purification of functional AQP4 water channels. Initial experiments were done with an AQP4 fusion protein containing an N-terminal polyhistidine tag to permit purification by metal-ion affinity chromatography. It was found that although $(his)_6$AQP4 was expressed in substantial quantities and was apparently targeted to the Sf9 cell plasma membrane, water permeability in Sf9 cell plasma membranes was increased little over that in noninfected cells. The polyhistidine tag may interfere with AQP4 protein folding or assembly into orthogonal arrays (18), or the tag might directly block the AQP4 water pore. The untagged AQP4 protein was expressed strongly at the Sf9 cell plasma membrane as demonstrated by immunocy-

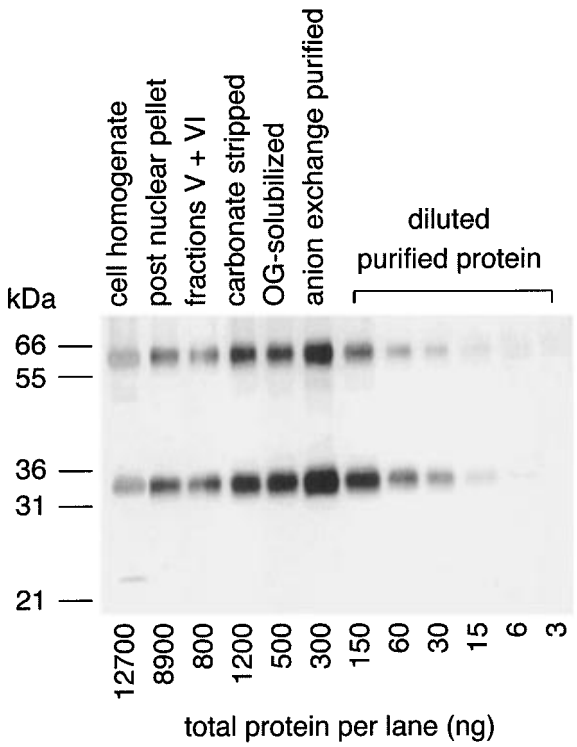

FIGURE 6: AQP4 immunoblot of materials at each stage of purification. Indicated samples were resolved by SDS−PAGE (see Table 1). In addition, serial dilutions of the final purified protein were studied to determine antibody detection efficiency. The total protein run in each lane is indicated.

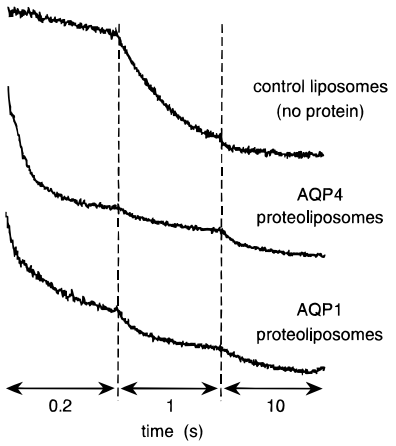

FIGURE 7: Functional analysis of proteoliposomes reconstituted with purified AQP4. Liposomes not containing protein and proteoliposomes reconstituted with AQP4 (protein-to-lipid ratio 0.05 w/w) or AQP1 (protein-to-lipid ratio 0.062 w/w) were prepared as described under Methods. Liposomes were subjected to a 30 mM inwardly directed sucrose gradient in the stopped-flow apparatus at 10 °C.

tochemistry and membrane fractionation. Purification was achieved by membrane fractionation, membrane stripping, detergent solubilization, and anion exchange chromatography. Significant enrichment (78-fold) was achieved by membrane fractionation, which removed soluble protein, nuclei, mitochondria, and endoplasmic reticulum, the major low-density membrane contaminant. An additional 3.5-fold purification was achieved by carbonate stripping of nonintegral proteins and detergent solubilization, which each selected for AQP4. Finally, it was found that AQP4 bound strongly to an anion exchange resin, permitting purification to near-homogeneity (enrichment factor of 1300) under nondenaturing conditions. AQP4 had very different biochemical properties from AQP1 in terms of solubility and chromatographic properties. For example, AQP4 was efficiently extracted from membranes by low concentrations of the anionic detergent *N*-laurylsarcosine, whereas AQP1 remains membrane-associated (*28*). Reconstitution of functional AQP4 water channels required a reducing environment whereas reconstitution of AQP1 did not.

Functional measurements of water permeability in reconstituted proteoliposomes showed very high water permeability, low activation energy, and a single channel water permeability ~3-fold greater than that for AQP1. Water permeability was also very high, weakly temperature-dependent, and mercurial-insensitive in plasma membrane vesicles from AQP4-expressing Sf9 cells. The water permeability coefficient of 0.053 cm/s was substantially greater than that in native membranes from mammalian cells. Transport of urea and glycerol was slow and not different from that in membranes from control Sf9 cells. Estimating that AQP4 comprises ~3% of membrane mass (since AQP4 is 6% of protein in fractions 5+6 per Table 1, and assuming that the membrane is 50% protein by weight), the plasma membrane P_f is 0.057 cm/s, and the computed AQP4 surface density is ~2800 monomers per μm^2, the single channel water permeability (p_f) was $\sim 19 \times 10^{-14}$ cm^3/s per AQP4 monomer. This value agrees with that of 15×10^{-14} cm^3/s measured in AQP4 proteoliposomes and suggests that most or all AQP4 molecules are functional.

The high single channel water permeability for AQP4 suggests that simple pore models may not be adequate to describe water movement through molecular aquaporins. For a right cylindrical pore that transports water by a single-file mechanism, $r_o^2 = p_f L/\pi D_w$ (*29*), where r_o is the pore radius, L is the pore length, and D_w is the diffusion coefficient of a single water molecule in the pore (2.4×10^{-5} cm^2/s). Assuming that each aquaporin protein monomer contains a 4-nm-long right cylindrical water pore, a pore diameter of 0.38 nm was computed for AQP1 based on its p_f of 6.8×10^{-14} cm^3/s (*30*). The AQP4 p_f of 15×10^{-14} cm^3/s determined here predicts a pore diameter of 0.56 nm, which would permit the transport of small solutes. The simplistic equations derived for idealized cylindrical, noninteractive water pores are therefore probably inadequate to provide useful information about molecular aquaporins. A molecular simulation approach will be required to model aquaporin function (when atomic resolution structural data are available) as well as the possible enhancement of water flow related to orthogonal array assembly.

Insect baculoviruses have been used for several years for the heterologous expression of eukaryotic proteins in Sf9 cells under the control of the strong viral polyhedrin gene promoter. The baculovirus system has been used extensively to express soluble proteins, and more recently to express functional membrane transporters and channels, including the cardiac Na^+-Ca^{2+} exchanger (*31*), Na^+/glucose cotransporter (*32*), CFTR Cl^- channel (*33*), and renal Na^+/phosphate cotransporter (*34*). The insect cell system is in general superior to bacterial and yeast expression systems for protein processing and posttranslational modifications, particularly for membrane proteins. However, membrane protein yields from insect cells are often substantially lower than yields for soluble proteins, possibly because of inefficient recognition of heterologous signal peptides by the insect cell protein

translocation machinery (*35*), cell toxicity (*36*), and/or the limited amount of membrane available for protein insertion. The molar yield of AQP4 protein per liter of Sf9 cell culture was similar to that found for two other membrane proteins that were successfully purified from Sf9 cells—CFTR (~3 mg/L of culture, reference *33*) and the human α1 glycine receptor (0.33 mg/L, reference *37*). The expressed AQP4 protein was functional and suitable to establish a purification protocol. The milligram quantities of AQP4 generated from Sf9 cells should permit examination of AQP4 structure by spectroscopic and crystallographic methods. Based on preliminary studies of AQP2 and AQP3 expression in Sf9 cells (data not shown), the insect cell expression system is suitable for functional expression and purification of other members of the aquaporin family.

ACKNOWLEDGMENT

We thank Drs. D. C. A. Neville and R. R. Townsend for help with the mass spectrometry analysis, which was supported by NIH Grant RR01614 awarded to the UCSF Mass Spectrometry Facility (A. L. Burlingame, director).

REFERENCES

1. Knepper, M. A. (1994) *Proc. Natl. Acad. Sci. U. S. A. 91*, 6255−6258.
2. Van Os, C. H., Deen, P. M. T., and Dempster, J. A. (1994) *Biochim. Biophys. Acta 1197*, 291−309.
3. Agre, P., and Nielsen, S. (1995) *Kidnet Int. 24*, 1057−1068.
4. Verkman, A. S., Van Hoek, A. N., Ma, T., Frigeri, A., Skach, W. R., Mitra, A., Tamarappoo, B. K., and Farinas, J. (1996) *Am. J. Physiol. 270*, C12−C30.
5. Reizer, J., Reizer, A., and Saier, M. H. (1993) *Crit. Rev. Biochem. Mol. Biol. 28*, 235−257.
6. Fushimi, K., Uchida, S., Hara, Y., Hirata, Y., Marumo, F., and Sasaki, S. (1993) *Nature 361*, 549−552.
7. Deen, P. M., Verkijk, M. A., Knoers, N. V., Wieringa, B., Monnens, L. A., Van Os, C. H., and Van Oost, B. A. (1994) *Science 264*, 92−95.
8. Frigeri, A., Gropper, M., Turck, C. W., and Verkman, A. S. (1995) *Proc. Natl. Acad. Sci. U.S.A. 92*, 4328−4331.
9. Verbavatz, J. M., Brown, D., Sabolic, I., Valenti, G., Ausiello, D. A., Van Hoek, A. N., Ma, T., and Verkman, A. S. (1993) *J. Cell Biol. 123*, 605−618.
10. Preston, G. M., and Agre, P. (1991) *Proc. Natl. Acad. Sci. U.S.A. 88*, 11110−11114.
11. Van Hoek, A. N., Wiener, M. C., Verbavatz, J. M., Brown, D., Townsend, R. R., Lipniunas, P. H., and Verkman, A. S. (1995) *Biochemistry 34*, 2212−2219.
12. Shi, L.-B., Skach, W. R., and Verkman, A. S. (1994) *J. Biol. Chem. 269*, 10417−10422.
13. Mitra, A. K., Van Hoek, A. N., Wiener, M. C., Verkman, A. S., and Yaeger, M. (1995) *Nat. Struct. Biol. 2*, 726−729.
14. Walz, T., Typke, D., Smith, B. L., Agre, P., and Engel, A. (1995) *Nat. Struct. Biol. 2*, 730−732.
15. Jap, B. K., and Li, H. L. (1995) *J. Mol. Biol. 251*, 413−420.
16. Hasegawa, H., Ma, T., Skach, W., Matthay, M., and Verkman, A. S. (1994) *J. Biol. Chem. 269*, 5497−5500.
17. Shi, L.-B., and Verkman, A. S. (1996) *Biochemistry 35*, 538−544.
18. Yang, B., Brown, D., and Verkman, A. S. (1996) *J. Biol. Chem. 271*, 4577−4580.
19. Zeuthen, T., and Stein, W. D. (1994) *J. Membr. Biol. 137*, 179−195.
20. Yang, B., Ma, T., and Verkman, A. S. (1995) *J. Biol. Chem. 270*, 22907−22913.
21. Frigeri, A., Gropper, M., Umenishi, F., Kawashima, M., Brown, D., and Verkman, A. S. (1995) *J. Cell Sci. 108*, 2993−3002.
22. Shi, L. B., Skach, W. R., Ma, T., and Verkman, A. S. (1995) *Biochemistry 34*, 8250−8256.
23. Ma, T., Yang, B., Gillespie, A., Carlson, E. J., Epistein, C. J., and Verkman, A. S. (1997) *J. Clin. Invest.* (in press).
24. Laize, V., Rousselet, G, Verbavatz, J. M., Berthonaud, V., Gobin, R., Roudier, N., Abrami, L., Ripoche, P., and Tacnet, F. (1995) *FEBS Lett. 373*, 269−274.
25. Umenishi, F., and Verkman, A. S. (1996) *J. Am. Soc. Nephrol. 7*, 1274.
26. Jung, J. S., Bhat, R. V., Preston, G. M., Guggino, W. B., Baraban, J. M., and Agre P. (1994) *Proc. Natl. Acad. Sci. U.S.A. 91*, 13052−13056.
27. Ma, T., Frigeri, A., Tsai, S. T., Verbavatz, J. M., Verkman, A. S. (1993) *J. Biol. Chem. 268*, 22756−22764.
28. Van Hoek, A. N., Verkman, A. S. (1992) *J. Biol. Chem. 267*, 18267−18269.
29. Finkelstein, A. (1987) *Water movement through lipid bilayers, pores, and plasma membranes: theory and reality*, p 45, Wiley and Sons, New York.
30. Zhang, R., Skach, W. R., Hasegawa, H., van Hoek, A. N., Verkman, A. S. (1993) *J. Cell Biol. 120*, 359−369.
31. Li, Z., Smith, C. D., Smolley, J. R., Bridge, J. H. B., Frank, J. H., and Philipson, K. D. (1992) *J. Biol. Chem. 267*, 7828−7833.
32. Smith, C. D., Hirayama, B. A., and Wright, E. M. (1992) *Biochim. Biophys. Acta 1104*, 151−159.
33. O'Riordan, C. R., Erickson, A., Bear, C., Li, C., Manavalan, P., Wang, K. W., Marshall, J., Scheule, R. K., McPherson, J. M., Cheng, S. H., and Smith, A. E. (1995) *J. Biol. Chem. 270*, 17033−17043.
34. Fucentese, M., Winterhalter, K., Murer, H., and Biber, J. (1995) *J. Membr. Biol. 144*, 43−48.
35. Harvis, D., Summers, M. D., Garcia, A., and Bohlmeyer, D. A. (1993) *J. Biol. Chem. 26*, 16754−16762.
36. Gimpl, G., Klein, U., Reilander, H., and Farenholz, F. (1995) *Biochemistry 34*, 13794−13801.
37. Cascio, M., Schoppa, N. E., Grodzicki, R. I., Sigworth, F. J., and Fox, R. O. (1993) *J. Biol. Chem. 268*, 22135−22142.
38. Velardo, M. A., Brettauer, R. K., Boutard, A., Reinhold, B., Reinhold, V. N., and Castelliino, F. J. (1993) *J. Biol. Chem. 268*, 17902−17907.

BI970231R